

# Anthropic Pollution Impacts on Groundwater Vulnerability Based on Modified DRASTIC-FAHP

Mohammad Reza Goodarzi (✉ [Goodarzimr@yazd.ac.ir](mailto:Goodarzimr@yazd.ac.ir))

Yazd University <https://orcid.org/0000-0002-6296-2315>

Amirreza R. Niknam

Yazd University

Vahid Jamali

Yazd University

Hamid Reza Pourghasemi

Shiraz University School of Agriculture

Mahboobeh Kiani-Harchegani

Yazd University

---

## Research Article

**Keywords:** Vulnerability, Groundwater, Modified DRASTIC, Fuzzy-AHP, Nitrate contamination, Iran

**Posted Date:** March 10th, 2021

**DOI:** <https://doi.org/10.21203/rs.3.rs-245669/v1>

**License:**  This work is licensed under a Creative Commons Attribution 4.0 International License.

[Read Full License](#)

---

# Anthropic pollution impacts on groundwater vulnerability based on modified DRASTIC-FAHP

Mohammad Reza Goodarzi<sup>1,\*</sup>, Amirreza R.Niknam<sup>2</sup>, Vahid Jamali<sup>2</sup>, Hamid RezaPourghasemi<sup>3</sup>, Mahboobeh Kiani-Harchegani<sup>4</sup>

1) Assistant professor, Department of Civil Engineering, Yazd University, Yazd, Iran. E-mail: Goodarzimr@yazd.ac.ir

2) MSc student, Department of Civil Engineering, Water Resources Management Engineering, Yazd University, Yazd, Iran. E-mail: arshamrajabpour@gmail.com and couv.jamali@gmail.com

3) Associate professor, Department of Natural Resources and Environmental Engineering, College of Agriculture, Shiraz University, Shiraz, Iran. E-mail: hr.pourghasemi@shirazu.ac.ir

4) Postdoc, Department of Watershed Management Engineering, Faculty of Natural Resources, Yazd University, Yazd Province, Iran. E-mail: mahboobeh.kiyani20@gmail.com

## Acknowledgement

The authors would like to thank Dr. Michael Fioren at the USGS Wisconsin Water Science Center for revising of language of manuscript.

## Abstract

In arid and semi-arid regions such as Iran, groundwater is more important for humans and ecosystems than surface water. Different models of groundwater vulnerability assessment can be used to better manage water resources. The purpose of this study is to evaluate the qualitative vulnerability of groundwater resources in the Birjand Plain aquifer using the DRASTIC model and 7 hydrogeological components. DRASTIC model was also modified by adding land use component (MDRASTIC) based on Analytical Hierarchy Process (AHP) and Fuzzy Analytic Hierarchy Process (FAHP) methods. After calculating the vulnerability index, the vulnerability of each method was mapped and the final index obtained from each method was classified into 4 different categories. Nitrate concentration was used to confirm the results and to analyze the sensitivity of a single parameter. Sensitivity analysis showed that the groundwater vulnerability is mainly affected by water depth and land use. To validate each of the models, their correlation with nitrate concentration was calculated and compared. To determine the correlation coefficient, simple linear regression method was performed and the Pearson and Spearman methods were used. According to the obtained Pearson correlation results, the DRASTIC, MDRASTIC, MDRASTIC-AHP, and

34 MDRASTIC-FAHP models resulted in values of 0.550, 0.680, 0.778, and 0.794 respectively. The results show a  
35 good correlation between the modified DRASTIC-FAHP model and nitrate concentration as an indicator of  
36 groundwater pollution.

37

38 **Keywords:** Vulnerability, Groundwater, Modified DRASTIC, Fuzzy-AHP, Nitrate contamination, Iran

39

## 40 **1. Introduction**

41 All communities need a clean and plentiful source of water for drinking, health, agriculture, industry, and energy  
42 production (Maqsoom et al., 2020). In arid and semi-arid areas where surface water is less available, groundwater  
43 can be the main source of water supply due to its large volume and less vulnerability to pollution. Iran is a country  
44 where most of its area is made up of arid and semi-arid regions. Both qualitatively and quantitatively, water  
45 pollution problems have been worsening. Due to rapid and widespread increase in population, irregular planning,  
46 urban sprawl, different land use classification patterns and system, improper sewage disposal systems including  
47 sewage from industry, agriculture, and urban areas, water pollution problems have been alarming. (Singha et al.,  
48 2017; Kumar et al., 2018). Groundwater pollution treatment methods are very complex and it is also difficult to  
49 determine the level of pollution on a regional scale (Bai et al., 2012). Groundwater vulnerability assessment methods  
50 divide an area into different sub-areas in terms of susceptibility to pollution (Guo et al., 2006). Using this  
51 information, protective measures can be prioritized to the most vulnerable. Various models to assess aquifer  
52 vulnerabilities are available including DRASTIC (Aller and Robert, 1985), AVI (Stempvoort et al., 1993),  
53 SINTACS (Vrba et al., 1994), EPIK (Doerflinger and Zwahlen, 1997), and GODS (Foster et al., 2002). Of all the  
54 above models, DRASTIC, due to its simplicity and flexibility, has been used more than other models to assess  
55 groundwater pollution (Pacheco et al., 2015; Tiwari et al., 2016; Neshat and Pradhan, 2017). This model was  
56 developed by the United States Environmental Protection Agency (USEPA). Karami Shahmaleki et al. (2013)  
57 showed that the Analytical Hierarchy Process (AHP) method is more accurate than the combined logistic regression  
58 and modified DRASTIC methods for assessing aquifer vulnerability in the Dezful-Andimeshk. Shirazi et al. (2013)  
59 assessed the sensitivity to groundwater in Malacca state in Malaysia using GIS and DRASTIC methods and  
60 prepared a map to assess groundwater sensitivity based on land use. Mahmoudzadeh et al. (2013) studied the  
61 vulnerability of Isfahan-Meimeh Aquifer also in Iran using three methods including, DRASTIC, GODS, and AVI.  
62 The results of this study indicate the completeness of the DRASTIC methods for aquifer vulnerability. Sener and  
63 Sener (2015) used fuzzy-AHP DRASTIC to prepare a vulnerability map presenting DRASTIC characteristic  
64 coefficients calculated using FAHP and the value of the vulnerability index of the region. Sinha et al. (2016)  
65 Investigated the vulnerability of the Kharun Basin using a modified DRASTIC model. The final results showed a  
66 vulnerability index between 86 and 191. Also, using sensitivity analysis, water depth, land use, and topography  
67 parameters were selected as the most effective parameters. Hussain et al. (2017) evaluated a stressed aquifer in the  
68 Kut Do area in the Punjab Plain in India using DRASTIC model. This area is of environmental concern due to the  
69 increase of uncontrolled agriculture and source of non-point pollution and salinity. Jesiya and Gopinath (2019)  
70 considered regional vulnerability using Fuzzy AHP DRASTIC-L method based on GIS in southern India. Modified

71 DRASTIC factors were rated using FAHP and finally the information was integrated by GIS tool and areas with  
72 high to very high vulnerabilities were identified. [Maqsoom et al. \(2020\)](#) studied the vulnerability of groundwater in  
73 the Gilgit area of Baltistan in northern Pakistan. Due to urban sprawl, groundwater resources in this area are  
74 declining. In this study, the GIS-based DRASTIC model was used and also because of the importance of human  
75 activities in the DRASTIC model they combined the effects of the human factor as a parameter (DRASTIC-A).  
76 Finally, comparison of the result with nitrate dispersion showed that the DRASTIC-A model has better results than  
77 DRASTIC.

78 For this aim, four GIS-based methods including, DRASTIC, modified DRASTIC, AHP, and FAHP were applied to  
79 map groundwater vulnerability in the research area. Also, for validation, the results obtained from four different  
80 methods were examined with nitrate concentration.

81  
82  
83

## 84 **2. Materials and methods**

### 85 **2.1. Study area**

86 The study area is Birjand Plain, which is located in the northern part of Bagheran highlands (latitudes 32° 34' to 33°  
87 8' N and longitudes 58° 41' to 59° 44' E) in Iran. The total area of Birjand Watershed is 3,425 square kilometers, of  
88 which about 980 square kilometers is composed of plain sand the rest is composed of mountains ([Fig. 1](#)). This plain  
89 is elongated and is surrounded by highlands and the central part consists of an alluvial aquifer ([Eftekhari et al.,  
90 2019](#)). It is bounded on the east by the Momenabad and Sistanhighlands, on the south by the Bagheran and Rech  
91 mountains, on the north by the Mol, Markuhhighlands, and on the west by the Karang and Chenghighlands. The  
92 Birjand plain is considered as an arid region according to climatic classifications. Annual rainfall is 177 mm and the  
93 altitude above sea level is 1,240 m ([Aryafar et al., 2020](#)).

94 **Fig. 1.**

95

### 96 **2.2. DRASTIC model**

97 DRASTIC is an acronym made up of the hydrogeologic parameters controlling groundwater pollution. These  
98 parameters include: depths to water (D), net recharge (R), aquifer media (A), soil media (S), topography (T), impact  
99 of vadose zone (I), and hydraulic conductivity (C) of aquifer. The DRASTIC model calculates a vulnerability index  
100 that is used to study groundwater pollution by hydrogeological parameters in different regions. The DRASTIC model  
101 results are calculated analytically and then processed using GIS. In the past few years, the DRASTIC model has  
102 been modified according to the characteristics of specific study areas by adding or removing various parameters ([Lee,  
103 2003](#); [Wang et al., 2007](#); [Simsek et al., 2006](#); [Umar et al., 2009](#); [Awawdeh and Jaradat, 2010](#); [Martinez-Bastida et  
104 al., 2010](#); [Şener and Şener, 2015](#); [Jesiya and Gopinath, 2019](#); [Maqsoom et al., 2020](#)). The classification range for  
105 each parameter—between 1 and 10—indicates the impact of each parameter on aquifer vulnerability. Weights from 1  
106 to 5 are then assigned to the seven DRASTIC parameters to indicate their relative importance ([Table 1](#)). Weights and

107 ratings were generated by [Aller and Robert \(1985\)](#) using the Delphi method. The DRASTIC index is calculated using  
108 Eq. (1):

$$DI = DrDw + RrRw + ArAw + SrSw + TrTw + IrIw + CrCw \quad (1)$$

109  
110 where,  $r$  are the ratings allocated to each parameter and  $w$  are the weights allocated to each parameter.  
111 Higher DRASTIC index values indicate higher vulnerability and lower DRASTIC index values indicate lower  
112 region vulnerability.

### 113 **Table 1**

#### 114 115 **2.2.1. Depth to water table**

116 Depth to water table is the depth that a pollutant must pass to reach groundwater so greater depth to water indicates  
117 less vulnerability. For areas with deeper water, more time is also available for pollution to decrease due to  
118 transformation or degradation of contaminants ([Maqsoom et al., 2020](#)). The classification of the depth to water table  
119 was 1 (minimum impact) to 10 (maximum impact) for input into DRASTIC. In general, deeper values correspond  
120 with lower DRASTIC rank values ([Abdelmadjid and Omar, 2013](#); [Natraj and Katyal, 2014](#); [Ghosh et al., 2015](#);  
121 [Tomer et al., 2019](#)). To prepare this layer, data related to 18 piezometers, located in different places of the plain,  
122 were collected through the regional water of southern-Khorasan Province, in a one-year period from October 2017  
123 to September 2018. ArcGIS 10.6 and interpolated using Kriging interpolation method in Spatial Analyst extension  
124 ([Eftekhari et al., 2019](#); [Tomer et al., 2019](#)) ([Fig. 2A](#)).

#### 125 126 **2.2.2. Net recharge**

127 Net recharge is the amount of water that infiltrates the surface and reaches the water table. This factor causes the  
128 vertical transfer of pollution to the water surface and its horizontal movement inside the aquifer ([Maqsoom et](#)  
129 [al., 2020](#)). The Piscopo method according to Equation 2 ([Piscopo, 2001](#)) was used to prepare the net recharge  
130 consisting of a total of three factors: slope, rainfall, and soil permeability. Rainfall maps were obtained using  
131 average annual rainfall data for years 2017 and 2018 prepared from the Birjand Meteorological Department. A slope  
132 map was obtained from Topographic map and digital elevation model, the detailed map resolution is 1:25000. Data  
133 and information related to soil permeability of Jihad Agricultural Office were also used to prepare the permeability  
134 map. [Table 2](#) shows the classification and evaluation of net recharge and a net recharge map is shown in [Fig. 2B](#).

$$135 \text{ Net recharge} = \text{soil permeability} + \text{rainfall} + \text{slope} (\%) \quad (2)$$

### 136 137 **Table 2**

#### 138 **2.2.3. Aquifer media**

139 Aquifer media indicates the hydrogeology of the groundwater system and affects groundwater recharging,  
140 contaminant displacement, etc. ([Remesan and Panda, 2008](#), [Jesiya and Gopinath, 2019](#)). To prepare the aquifer  
141 media zoning map, observation and operation well logs were used in the study area, obtained from the Regional

142 water Department of southern Khorasan Province. Inverse Distance Weighting (IDW), in the ArcGIS Spatial  
143 Analyst extension, was used to prepare the aquifer map in the ArcGIS 10.6 (Fig. 2C). This method was used because  
144 it has the less error than Kriging.

145  
146 **2.2.4. Soil media**  
147 Soil media refers to all the materials in the upper part of the unsaturated area, dominated by plant root infiltration and  
148 soil biological activities, which has a great impact on the rate of groundwater recharge (Baghapour et al., 2014;  
149 Noori et al., 2019). Soil properties such as permeability and soil texture can enable contamination in the aquifer (Kim  
150 and Hamm, 1999). The soil map of the Birjand aquifer, scaled at 1:50000, was obtained from the Jihad Agriculture  
151 Office of southern Khorasan. The map was scanned, digitized, rasterized and classified (Fig. 2D).

152  
153 **2.2.5. Topography**  
154 Topography refers to the slope of an area. Water is more likely to infiltrate in low-slope areas. In these areas, runoff  
155 is less, and the possibility of pollutant infiltration increases. Areas with steep slopes have less infiltration and large  
156 amounts of runoff and are therefore less vulnerable to groundwater pollution (Tomer et al., 2019). A slope map was  
157 prepared using DEM with a spatial resolution of 30 meters in ArcGIS 10.6 (Fig. 2E) (Eftekhari et al., 2019).

158  
159 **2.2.6. Impact of vadose zone**  
160 The impact of vadose zone on aquifer pollution is similar to soil media and depends on the permeability of the  
161 constituents and the characteristics of the unsaturated zone. To prepare this layer, logs of observation and operation  
162 of 22 wells obtained from the Regional Water Department of southern Khorasan Province, were interpolated using  
163 the IDW method in the ArcGIS 10.6 (Fig. 2F).

164  
165 **2.2.7. Hydraulic conductivity**  
166 Hydraulic conductivity refers to the ability of the aquifer to control the transfer of material. Aquifers with the  
167 highest hydraulic conductivity are most at risk of contamination (Tomer et al., 2019). To prepare this layer,  
168 Transmissivity data and information from pumping tests were obtained from the Regional Water Department of  
169 southern Khorasan Province. Then, according to the Transmissivity parameter measured in experiment and dividing  
170 it by the saturation thickness of the aquifer, hydraulic conductivity is obtained (Pathak et al., 2009). Finally,  
171 hydraulic conductivity mapping was prepared using IDW method (Fig. 2G).

172  
173 **Fig. 2.**  
174

175 **2.3. Modified DRASTIC**  
176 Adding a land use parameter to the DRASTIC model is the modified DRASTIC (MDRASTIC) model. The land use  
177 map in this study, with a scale of 1: 50,000, was obtained from the Regional Water Department of South Khorasan  
178 Province. Land use types in the study area include, gardens, agricultural areas, residential areas, grasslands, forests

179 and shrublands and river bed (Fig. 3) and were assigned DRASTIC ranks between 1 and 10. Incorporating land-use  
180 into DRASTIC resulted in a model referred to as MDRASTIC or DRASTIC-LU. The MDRASTIC index (MDI) was  
181 calculated using Eq. (3):

$$MDI = DrDw + RrRw + SrSw + TrTw + IrIw + CrCw + LUrLUw \quad (3)$$

182  
183 where,  $LUr$  is the rating of land use factor and  $LUw$  is the weight of the land use factor.

### 186 Fig. 3

#### 187 2.4. Modified DRASTIC-AHP

188 The Analytic Hierarchy Process (AHP) is a tool for efficiently analyzing complex decisions and thus helping the  
189 decision-maker choose the best possible option. This method was developed in 1980 by Thomas Saaty (Saaty, 1980)  
190 and applied in several fields. After calculating the weight of each parameter in the MDRASTIC method, the AHP  
191 tool was used to obtain new weights related to each parameter. Super decision software was used to prepare the  
192 weights of the parameters by AHP. Finally, for matrix compatibility, the consistency ratio (CR) value must be less  
193 than or equal to 0.1. If unsuccessful, the comparison answers should be re-examined (Sener and Davraz, 2012;  
194 Lakusic, 2019).

#### 196 2.5. Modified DRASTIC-FAHP

197 The AHP method results in good results, but, it cannot reflect the style of human thinking (Kahraman et al., 2003).  
198 To make more reliable decisions, Van laarhoven and Pedrycz (1983) proposed the Fuzzy Analytic Hierarchy  
199 Process (FAHP). The FAHP method, determines the weight of the criteria primarily according to the subjective  
200 judgments of experts through a two-to-two comparison. In this method, comparisons are made using triangular  
201 numbers whose expansion indicates the uncertainty of a particular judgment (Sener and Sener, 2015). In fact, it gives  
202 more credibility and confidence to the judgments of experts (Sener and Sener, 2015). After Van laarhoven and  
203 Pedrycz (1983), Chang developed a new method for fuzzy AHP management in 1996 (Chang, 1996) using  
204 triangular fuzzy numbers (TFN) for a two-by-two comparison scale of fuzzy AHP and limit analysis method. Paired  
205 comparison numbers of one parameter compared to another can be seen in the fuzzy AHP method in Table 3 (Sener  
206 and Sener, 2015; Tseng et al., 2008). The numbers  $2/3$ ,  $1$ ,  $3/2$ ,  $2$ ,  $5/2$ ,  $3$ ,  $7/2$ ,  $4$ , and  $9/2$  were used as fuzzy scaling  
207 ratios, related to preferring one parameter over another with distance values.

### 209 Table 3

210  
211 A fuzzy number may be expressed as a triangle or a trapezoid. In the triangular number (TFN), the corresponding  
212 number is expressed as  $M = (l, m, u)$ . Parameter  $l$  represents the lowest possible value,  $m$  represents the most  
213 probable value and  $u$  represents the highest possible value for the desired number, and the desired number can vary

214 between a and c(Şener and Şener, 2015). Kahraman et al. (2003) summarized the steps for calculating the relative  
 215 weight of each criterion in the FAHP method proposed by Chang's extent analysis as follows:  
 216 Step 1: Formation of paired comparison matrix using fuzzy numbers  
 217 Step 2: Calculation of S matrix for each of the paired comparison matrix rows.

$$S_i = \sum_{j=1}^m M_{g^i}^j \otimes \left[ \sum_{i=1}^n \sum_{j=1}^m M_{g^i}^j \right]^{-1} \quad (4)$$

218  
 219 In Eq. 4, M is a TFN inside the paired comparison matrix. In fact, when calculating the S matrix, each component of  
 220 the fuzzy number is multiplied by the sum, and in the fuzzy inverse, the sum is multiplied by the total (Eqs. 5-7).

$$\sum_{j=1}^m M_{g^i}^j = \left( \sum_{j=1}^m l_j, \sum_{j=1}^m m_j, \sum_{j=1}^m u_j \right), \quad j = 1, 2, \dots, m \quad (5)$$

$$\sum_{i=1}^n \sum_{j=1}^m M_{g^i}^j = \left( \sum_{i=1}^n l_i, \sum_{i=1}^n m_i, \sum_{i=1}^n u_i \right), \quad i = 1, 2, \dots, n \quad (6)$$

$$\left[ \sum_{i=1}^n \sum_{j=1}^m M_{g^i}^j \right] = \left( \frac{1}{\sum_{i=1}^n u_i}, \frac{1}{\sum_{i=1}^n m_i}, \frac{1}{\sum_{i=1}^n l_i} \right) \quad (7)$$

221  
 222 Step 3: The degree of possibility of M2 greater than equal to M1 is defined as follows:

$$V(M_2 \geq M_1) = \sup_{y \geq x} [\min(\mu_{M_1}(x), \mu_{M_2}(y))] \quad (8)$$

223  
 224 where x and y are the values on the axis of membership function of each criterion. Equation 8 can be expressed as  
 225 Eq. 9:

$$V(M_2 \geq M_1) = \text{hgt}(M_1 \cap M_2) = \mu_{M_2}(d) = \begin{cases} 1 & \text{if } m_2 \geq m_1 \\ 0 & \text{if } l_1 \geq u_2 \\ \frac{l_1 - u_2}{(m_2 - u_2) - (m_1 - l_1)} & \text{otherwise} \end{cases} \quad (9)$$

227

228 where,  $M1 = (l_1, m_1, u_1)$  and  $M2 = (l_2, m_2, u_2)$  are two triangular fuzzy numbers and  $d$  is the highest point of  
 229 intersection between  $\mu_{M1}$  and  $\mu_{M2}$ (Fig.4).

230 *Step 4:* In this step, the non-normalized weight vector was obtained by calculating the minimum value of  $V$   
 231 calculated in the previous step.

$$232 \quad \min V = (M \geq M_i), \quad i = 1, 2, \dots, k \quad (10)$$

$$d'(A_i) = \min V(S_i \geq S_k) \quad k = 1, 2, \dots, n; k \neq i \quad (11)$$

$$W' = (d'(A_1), d'(A_2), \dots, d'(A_n))^T A_i (i = 1, 2, \dots, n) \quad (12)$$

233  
 234 *Step 5:* The weight vector obtained from the previous step, which was not normalized, was normalized to obtain the  
 235 final weight vector, which is our ultimate goal in the fuzzy calculations

$$W = (d(A_1), d(A_2), \dots, d(A_n))^T \quad (13)$$

236  
 237 **Fig. 4**

## 238 2.6. Sensitivity analysis

239 Because the DRASTIC model supports large-scale data sets, uncertainty should be considered in improperly  
 240 assigning rating and weight at each step to mitigate wrong final output and impacts on the computational process of  
 241 the DRASTIC model. Sensitivity analysis allows providing valuable information about the values of ratings and  
 242 weights (Gogu and Dassargues, 2000; Edet 2014; Şener and Şener, 2015). In this study, the single-parameter  
 243 sensitivity analysis (SPSA) was performed.

## 244 2.7. Single parameter sensitivity analysis

245  
 246 This analysis was introduced by Napolitano and Fabbri (1996), to evaluate the effect of each of the parameters of the  
 247 MDRASTIC model in measuring vulnerability. The theoretical weight for each parameter was compared to the  
 248 effective weight which is calculated using Eq. 14:

$$249 \quad W = \left[ \frac{(P_r \times P_w)}{V} \right] \times 100 \quad (14)$$

250  
 251 where,  $W$  is the effective weight of each parameter,  $P_r$  and  $P_w$  are the ratings and weight related to that parameter,  
 252 respectively, and  $V$  is the total vulnerability index in that area.

254  
255  
256  
257  
258  
259  
260  
261  
262

## 2.8. Validation

Simple linear regression analysis (SLRA) was used to compare the results of the four DRASTIC methods to nitrate concentration parameter to evaluate the correlation. Pearson, Spearman correlation coefficients (Panagopoulos et al., 2006; Kumar and Pramod Krishna, 2019; Maqsoom et al., 2020) were also used to evaluate the degree of correlation between models and nitrate concentration parameter to select the best method. Pearson's correlation coefficient ( $r$ ) determines the correlation between two variables with distance and relative scales, assuming a normal distribution and varies between +1 and -1 (Chok, 2010). It was calculated using Eq. 15:

$$r = \frac{\sum_{i=1}^n (x_i - \bar{x})(y_i - \bar{y})}{\sqrt{\sum_{i=1}^n (x_i - \bar{x})^2} \sqrt{\sum_{i=1}^n (y_i - \bar{y})^2}} \quad (15)$$

263  
264  
265  
266  
267  
268  
269

Where  $r$  is the correlation coefficient,  $x_i$  represents values of the x-variable in a sample,  $\bar{x}$  represents mean of the values of the x-variable,  $y_i$  represents values of the y-variable in a sample and  $\bar{y}$  represents mean of the values of the y-variable. The Spearman's rank correlation coefficient is a nonparametric measure used to quantify the strength of a link between two sets of data (Laerd Statistics, 2018; Kumar and Pramod Krishna, 2019). It was calculated using Eq. 16:

$$\rho = 1 - \frac{\sum_{n=1}^n d^2}{n(n^2 - 1)} \quad (16)$$

270  
271  
272  
273  
274  
275  
276  
277  
278

Where  $\rho$  is the Spearman's rank correlation coefficient,  $d$  represents difference between the two ranks of each observation and  $n$  represents number of observations. Nitrate data used were collected by 22 wells in the study area. Excel was used for linear regression model (Abdullah et al., 2018) and SPSS 26 was used for Pearson, Spearman correlations (Asgari Moghaddam et al., 2016; Baghapour et al., 2016).

279  
280  
281  
282  
283

## 3. Results

### 3.1. DRASTIC

After obtaining the ratings and weights of each parameter (Table 4), the final vulnerability map was created using ArcGIS 10.6. A quantile classification method was used to classify vulnerability categories in the final map. The set of values available by this classification method is divided into groups with equal numbers of values (Sener et al.,

284 2009).The results of this model showed that 5% of the aquifer has a low vulnerability class (79-95), 38% has a  
285 medium vulnerability (96-112) , 46% has a high vulnerability (113-129) and 11% has a very high vulnerability (131-  
286 146) (Fig. 6(A)).

287

### 288 3.2. Modified DRASTIC

289 The MDRASTIC index was calculated using Eq. 3 and a vulnerability map was generated using ArcGIS 10.6. The  
290 resulting map was divided into four vulnerable areas using a quantile classification method that varied from low to  
291 very high. TheMDRASTIC model, incorporating land use as a parameter resulted in a different distribution of  
292 vulnerability indices the standard DRASTIC method.The results of the MDRASTIC model showed that 4% of the  
293 Birjand aquifer has a low vulnerability class (90-113),59% has a medium vulnerability (114-137), 29% has a high  
294 vulnerability (138-161) and 8% has a very high vulnerability (162-185) (Fig. 6(B)).

295

### 296 3.3. Modified DRASTIC-AHP

297 The value of compatibility ratio (CR) was 0.023, which indicates the correctness of the comparisons (Fig. 5).  
298 According to the new weights, layers of each parameter were created in the GIS environment, and finally, a  
299 vulnerability map was prepared. The results of the MDRASTIC-AHPmethod showed that 4% of the Birjand  
300 aquiferhas a low vulnerability class (3.4-4.1), 52% has a medium vulnerability (4.2-4.9), 39% has a high  
301 vulnerability (5-5.7) and 5% has a very high vulnerability (5.8-6.5) (Fig.6(C)).

302

**Table 4**

303

**Fig. 5**

304

### 305 3.4. Modified DRASTIC-FAHP

306 MDRASTIC F-AHP vulnerability index was also obtained using the rating and weight determined for each  
307 parameter by the F-AHP method (Eq.4). The groundwater vulnerability map was also generated using the modified  
308 weights and ArcGIS 10.6 and it was divided into four vulnerable areas using a quantile classification method that  
309 varied from low to very high. The results of MDRASTIC-FAHP method showed that 2.8% of the aquifer area has a  
310 low vulnerability class (0.09-0.162), 53.2% has a moderate vulnerability (0.163-0.235), 40.3% has a high  
311 vulnerability (0.236-0.308) and 3.7% has a very high vulnerability (0.309-0.381) (Fig.6(D)).

312

313

**Fig. 6**

314

### 315 3.5. Single parametric sensitivity analysis

316 Statistical results of SPSA were presented for the DRASTIC model. Comparison of the theoretical weight of each  
317 parameter with the effective weight assigned to it in the aquifer of the studied plain showed that the theoretical and  
318 effective weights of each of the parameters of the DRASTIC model are not completely consistent. According to  
319 Table 5, the depth to water table parameter with an average effective weight of 23.6 is the most sensitiveparameter  
320 in assessing vulnerability. The theoretical weight determined by the DRASTIC model is less than the average  
321 effective weight of this parameter. Also, land use, aquifer media, the impact of vadose zone and hydraulic

322 conductivity have a more effective weight than the theoretical weight assigned to them in the DRASTIC model. It  
323 can also be seen from the sensitivity analysis that the net recharge and topography parameters have the least effect  
324 on groundwater vulnerability.

### 325 **Table 5**

### 326 327 **3.6. Validation**

328 The relationship between nitrate concentration and vulnerability indices obtained from different DRASTIC methods  
329 was used to evaluate and select the best method, based on the assumption that the most vulnerable areas in the  
330 aquifer should also experience the highest nitrate concentrations. Using nitrate field data obtained from 22 wells in  
331 the Birjand aquifer, the vulnerability map was confirmed (Fig. 7). Human and agricultural activities result in  
332 elevated concentration of nitrate in groundwater. Fig. 8 shows simple linear regression analysis diagrams to examine  
333 the correlation between the calculated indices and the values of groundwater nitrate concentration. The closer the  $R^2$   
334 values are to 1, the greater the correlation of the method. Also, to confirm and select the best method, the resulting  
335 vulnerability maps were evaluated using Pearson and Spearman correlation methods in SPSS 26 (Table 6). The  
336 results presented in Table (6) show a higher correlation of the FAHP vulnerability map with the nitrate  
337 concentration.

### 338 339 **Fig. 7.**

### 340 **Fig. 8.**

### 341 **Table 6.**

### 342 343 **4. Discussion**

344 Assessing and preventing groundwater contamination is essential for better and more efficient management of these  
345 resources. In this regard, various methods such as DRASTIC can be used to integrate different thematic layers to  
346 evaluate groundwater vulnerability in the desired area. The DRASTIC model considers 7 hydrogeological  
347 parameters and classifies them on a ten-grade scale. Finally, the parameters are combined in Eq1 to calculate a  
348 vulnerability index. The depth that a pollutant must travel to reach groundwater is called the depth to water table, or  
349 in fact, it can be said that the contaminant must travel after infiltrating the ground to reach the groundwater level. In  
350 this study, depth was divided into three intervals, namely, 9-15, 15-23, and > 30.4 meters. Factors that combine to  
351 parameterize net recharge include soil permeability, slope, and precipitation. (Piscopo, 2001). To prepare the net  
352 recharge map, a slope map was generated using DEM, rain data collected from Birjand Meteorological Department,  
353 and soil permeability data collected from Jihad Agricultural Office were considered as input data. Ranges and classes  
354 are listed in Table 2. The aquifer media in the DRASTIC model shows the intrinsic hydrogeology of the  
355 subsurface. Subsurface hydrogeologic processes such as groundwater recharge, contaminant displacement, etc., are  
356 influenced by the characteristics of the aquifer media (Remesan and Panda, 2008). The wells data collected from the  
357 Regional water Department of southern Khorasan Province to prepare the aquifer map. The Birjand aquifer was  
358 divided into two major geological formations. The part of the aquifer that contains sand and gravel coarse-grained  
359 deposits is assigned a higher rating of 9. Soil textures determine the potential for groundwater vulnerability and

360 control the movement of pollutants from the surface to the water table by soil grain size (Remesan and Panda, 2008).  
361 The permeability parameter was used to rating different soil types (Table 1). Four types of soil were identified in the  
362 Birjand aquifer. The highest rating was assigned to highly permeable soil (gravel) and the lowest value was assigned  
363 to soil with less permeability (loam). (Karthikeyan and Lakshmanan, 2012). The topography of an area refers to the  
364 characteristics of the surface and slope. Areas with lower slopes are more prone to pollution. The lower the slope,  
365 the less runoff and the greater the infiltration (Al-Adamat et al., 2003). A slope map was prepared using a digital  
366 elevation model (DEM) with spatial resolution of 30 meters and was divided into three classes: 0-2, 2-6 and 6-12  
367 percentage. In this site, nearly flat areas were allocated a high rating value of 10, and the steepest slopes receiving  
368 the lowest rating of 5. The vadose area includes the unsaturated area between the topsoil (soil cover) and the water  
369 table. The permeability of the materials of this layer has a great impact on the transmission of contamination.  
370 According to Aller and Robert (1985), and based on the geological description of the research area, the vadose zone  
371 was divided into three classes. The ability of the aquifer to transfer water that is constantly flowing in it is called  
372 hydraulic conductivity (Saha and Alam, 2014). Aquifers with the highest levels of hydraulic conductivity are most at  
373 risk of contamination (Tomer et al., 2019). The value of hydraulic conductivity ranged between 4.32 and 43.2 m/day,  
374 for the study area.

375 A final vulnerability map was created in ArcGIS 10.6 after determining the weight and rating of each parameter.  
376 The DRASTIC vulnerability index was calculated by combining the effects of each of the seven layers which  
377 calculated using ArcGIS 10.6 and according to Eq. 1. The value of this index is between 79 and 146 and it was  
378 classified into four categories of low to very high vulnerability to groundwater pollution (Fig. 6A). A quantile  
379 classification method was used to classify vulnerability categories in the final map. The high vulnerability was  
380 driven chiefly by the shallow water level, high hydraulic conductivity, and porous Vadose area, or the effect of all  
381 three together.

382 In most studies, the conventional DRASTIC model has been used to investigate the vulnerability of groundwater to  
383 pollution. The DRASTIC model considers the transfer of pollutants to groundwater through the unsaturated zone but  
384 does not take into account the pollution caused by anthropogenic effects and this can result in unrealistically low  
385 DRASTIC index (Shirazi et al., 2013). The anthropogenic activities are found in different forms in different study  
386 areas. For example, in this study, anthropogenic effects have been considered in the form of land use, such as  
387 agricultural areas or residential areas, etc. For this purpose, the land use parameter was added to the original  
388 DRASTIC model. The rating and weight of the anthropogenic impact map were determined according to the land  
389 use class contracts (Al-Adamat et al., 2003; Maqsoom et al., 2020) to produce a vulnerability map of  
390 MDRASTIC (Fig. 6B). The parameters that had the least impact on groundwater pollution include soil media, aquifer  
391 media, and topography while water depth table, land use, and hydraulic conductivity had the greatest impact among  
392 the parameters. The MDRASTIC map is classified into four vulnerability categories (very high, high, medium and  
393 low). Most of the study area was located in a highly vulnerable area. High vulnerability is observed in areas around  
394 gardens, agricultural areas and residential areas. To provide a better and more realistic method for classifying  
395 groundwater vulnerability, the MDRASTIC model parameters were modified using a analytic hierarchical process  
396 (AHP) (Sener and Davraz, 2012). Using the parameters of the MDRASTIC model, a comparison matrix was

397 generated and new weights and ratings were calculated for each parameter. Super decision software was used to  
398 prepare the weight of the parameters by Analytic Hierarchy Process. The results of the MDRASTIC-AHP Vulnerability  
399 Map showed that the western and southwestern regions are more prone to contamination. Low pollution potential  
400 areas in southern and eastern part which consists mostly of grasslands and forests was determined. To ensure better  
401 decisions and results, the weights of all eight parameters of the MDRASTIC vulnerability index were also modified  
402 with the help of weights obtained from the FAHP (Table 4). After that, each of the parameters was evaluated and  
403 paired comparisons by themselves and their rates were corrected. At each stage, after obtaining new weights, the  
404 compatibility ratios of the comparison matrices were obtained using Gogus and Boucher methods (1997). Using GIS  
405 tool, the final vulnerability map was prepared. After preparing the vulnerability results, it was found that the  
406 pollution potential in the southwestern regions is very high. There is uncertainty and ambiguity in the DRASTIC  
407 model because the classification of each parameter is graded based on the opinions of experts. To reduce this  
408 problem, the results of DRASTIC models zoning maps are confirmed by comparing the sensitive areas of the  
409 Birjand aquifer with the available nitrate concentration. Then, each parameter is analyzed separately for sensitivity.

410

## 411 **5. Conclusion**

412 In this study, using the experimental model of DRASTIC in GIS environment, the sensitivity of water to pollution in  
413 the aquifer of Birjand Plain was evaluated. In addition, land use patterns were used to create a better model called  
414 MDRASTIC or DRASTIC-LU. Due to the importance of weight values of DRASTIC parameters, AHP and FAHP  
415 methods were used to determine the weight values parameters. After calculating the vulnerability index, a  
416 vulnerability map of each method was prepared. To better understand and also show the vulnerability of the region,  
417 the final index obtained from each method was classified into four different classes. The results of the sensitivity  
418 analysis show that depth to the water table and land use have the most impact on vulnerability assessment in the  
419 Birjand aquifer, while net recharge and topography are the parameters that have the least impact in the study area. In  
420 order to verify the built methods, the relationship between the vulnerability index and the values of nitrate  
421 concentration obtained from 22 groundwater samples has been investigated. To determine the correlation  
422 coefficient, simple linear regression method was used in Excel and Pearson, Spearman methods were used in SPSS  
423 26. The results obtained from the correlation coefficient show that the MDRASTIC-FAHP method has the highest  
424 correlation with nitrate concentration values.

425

426

## 427 **Declarations**

428

429 Ethics approval and consent to participate

430 *Not applicable*

431

432 Consent for publication

433 *Not applicable*

434

435 Availability of data and materials

436 *Due to the nature of this research, participants of this study did not agree for their data to be shared publicly, so*  
437 *supporting data is not available.*

438  
 439 Competing interests  
 440 *The authors declare that they have no competing interests*  
 441

442 Funding  
 443 *No funding was received for this work*  
 444

445 Author contributions  
 446 *An author must take responsibility for at least one component of the work, should be able to identify who is*  
 447 *responsible for each other component, and should ideally be confident in their co-authors' ability and integrity.*  
 448

Component of the research	Author's name
Conceptualization	Mohammad Reza Goodarzi - Amirreza R. Niknam - Hamid Reza Pourghasemi
Methodology	Mohammad Reza Goodarzi - Amirreza R. Niknam - Vahid Jamali
Software	Mohammad Reza Goodarzi - Amirreza R. Niknam - Vahid Jamali
Validation	Mohammad Reza Goodarzi - Amirreza R. Niknam - Hamid Reza Pourghasemi - Mahboobeh Kiani-Harchegani
Formal analysis	Mohammad Reza Goodarzi - Amirreza R. Niknam - Hamid Reza Pourghasemi
Investigation	Mohammad Reza Goodarzi - Amirreza R. Niknam - Vahid Jamali
Resources	Mohammad Reza Goodarzi - Amirreza R. Niknam
Data Curation	Mohammad Reza Goodarzi - Amirreza R. Niknam
Writing - Original Draft	Mohammad Reza Goodarzi - Amirreza R. Niknam - Mahboobeh Kiani-Harchegani
Writing - Review & Editing	Mohammad Reza Goodarzi - Amirreza R. Niknam - Hamid Reza Pourghasemi - Mahboobeh Kiani-Harchegani
Supervision	Mohammad Reza Goodarzi - Hamid Reza Pourghasemi

449  
 450  
 451 **References**  
 452 Abdelmadjid B, Omar S (2013) Assessment of groundwater pollution by nitrate using intrinsic vulnerability  
 453 methods: A case study of the Nil valley groundwater (Jijel, North-East Algeria), Afr. J. Environ. Sci.  
 454 Technol. 7 (10): 949-960.  
 455 Abdullah TO, Ali SS, Al-Ansari NA, Knutsson S (2018) Possibility of Groundwater Pollution in Halabja Saidasadiq  
 456 Hydrogeological Basin, Iraq Using Modified DRASTIC Model Based on AHP and Tritium Isotopes.  
 457 Geosci. 8(7): 236.

458 Aller L, Robert S (1985) DRASTIC: A Standardized System for Evaluating Ground Water Pollution Potential Using  
459 Hydrogeologic Settings, Kerr Environmental Research Laboratory, Office of Research and Development,  
460 U.S. Environmental Protection Agency.

461 Al-Adamat RAN, Foster IDL, Baban SMJ (2003) Groundwater vulnerability and risk mapping for the Basaltic  
462 aquifer of the Azraq basin of Jordan using GIS, Remote sensing and DRASTIC. *Appl Geogr.* 23(4): 303-  
463 324.

464 Aryafar A, Khosravi V, Karami S (2020) Groundwater quality assessment of Birjand plain aquifer using kriging  
465 estimation and sequential Gaussian simulation methods. *Environ. Earth Sci.* 79(10): 210.

466 Asgari Moghaddam A, Nadiri A, Pakniya V (2016) Vulnerability Assessment of Bostan Abad Plain Qquifer by  
467 DRASTIC and SINTACS Models. *Hydrogeomorph.* 3(8): 21-52.

468 Awawdeh MM, Jaradat RA (2010) Evaluation of aquifers vulnerability to contamination in the Yarmouk River  
469 basin, Jordan, based on DRASTIC method. *Arab. J. Geosci.* 3(3): 273-282.

470 Baghapour MA, Talebbeydokhti N, Tabatabaei SH, Fadaei Nobandegani A (2014) Assessment of Groundwater  
471 Nitrate Pollution and Determination of Groundwater Protection Zones Using Drastic And Composite  
472 Drastic (cd) Models: The Case of Shiraz Unconfined Aquifer. *J. Health Sci. Surveill. Syst.* 2.--(2)

473 Baghapour MA, Fadaei Nobandegani A, Talebbeydokhti N, Bagherzadeh S, Nadiri AA, Gharekhani M, Chitsazan N  
474 (2016) Optimization of DRASTIC method by artificial neural network, nitrate vulnerability index, and  
475 composite DRASTIC models to assess groundwater vulnerability for unconfined aquifer of Shiraz Plain,  
476 Iran. *J. Environ. Health Sci. Eng.* 14(1): 13.

477 Bai L, Wang Y, Meng F (2012) Application of DRASTIC and extension theory in the groundwater vulnerability  
478 evaluation. *Water Environ. J.* 26(3): 381-391.

479 Chang D.-Y (1996) Applications of the extent analysis method on fuzzy AHP. *Eur. J. Oper. Res.* 95(3): 649-655.

480 Chok NS (2010) Pearson's Versus Spearman's and Kendall's Correlation Coefficients for Continuous Data. Master's  
481 Thesis.

482 Daly D, Drew D (1999) Irish methodologies for karst aquifer protection. *Hydrogeol Eng Geol Sinkholes Karst*  
483 *Balkema, Rotterdam.* 272\_267.

484 Doerfliger N, Zwahlen F (1997) EPIK: A new method for outlining of protection areas in karstic environment. In  
485 *International Symposium and Field Seminar on "Karst Waters and Environmental Impacts.* Gunay, G.,  
486 *Jonshon, A.I., Eds.; IAEA: Antalya, Turkey; Balkema, Rotterdam,* 117–123

487 Edet A (2014) An aquifer vulnerability assessment of the Benin Formation aquifer, Calabar, southeastern Nigeria,  
488 using DRASTIC and GIS approach. *Environ. Earth Sci.* 71(4): 1747-1765.

489 Eftekhari M, Akbari M, Ghezelsoufloo AA (2019) Qualitative Vulnerability Assessment of Birjand Plain Aquifer  
490 Using SINTACS Method. *J. Nat. Environ.* 72(3). (In Persian)

491 Foster S, Hirata R, Gomes D, Paris M, D'Elia M (2002) Groundwater quality protection - a guide for water utilities,  
492 municipal authorities and environment agencies (also in Spanish & Portuguese).

493 Ghosh A, Tiwari AK, Das S (2015) A GIS based DRASTIC model for assessing groundwater vulnerability of Katri  
494 Watershed, Dhanbad, India. *Model. Earth Syst. Environ.* 1 (3): 11.

495 Gogu RC, Dassargues A (2000) Sensitivity analysis for the EPIK method of vulnerability assessment in a small  
496 karstic aquifer, southern Belgium. *Hydrogeol. J.* 8(3): 337-345.

497 Gogus O, Boucher TO (1997) A consistency test for rational weights in multi-criterion decision analysis with fuzzy  
498 pairwise comparisons. *Fuzzy Set. Syst.* 86(2): 129-138.

499 Guo Q, Wang Y, Gao X, Ma T (2006) A new model (DRARCH) for assessing groundwater vulnerability to arsenic  
500 contamination at basin scale: a case study in Taiyuan basin, northern China. *Environ. Geo.* 52(5): 923-932.

501 Hussain Y, Ullah SF, Aslam AQ, Hussain MB, Akhter G, Martinez-Carvajal HE, Satgé F, Ashraf A, Iqbal, B,  
502 Cárdenas-Soto M (2017) Vulnerability assessment of an agro-stressed aquifer using a source-pathway-  
503 receptor model in GIS. *Model Earth Syst Environ.* 3(2): 595-604.

504 Jesiya NP, Gopinath G (2019) A Customized FuzzyAHP - GIS based DRASTIC-L model for intrinsic groundwater  
505 vulnerability assessment of urban and peri urban phreatic aquifer clusters. *Groundw. Sustain. Dev.* 8: 654-  
506 666.

507 Kahraman C, Cebeci U, Ulukan Z (2003) Multi-criteria supplier selection using fuzzy AHP. *Logist. Inf. Manag.*  
508 16(6): 382-394.

509 Karami Shahmaleki N, Behbahani SMR, Massah Bavani A, Khodaei K (2013) Comparison between  
510 LogisticRegression, Modified DRASTIC and AHP-DRASTIC Methods in Groundwater Vulnerability  
511 Assessment. *J. Environ. Stud.* 38(4): 79-92.

512 Karthikeyan B, Lakshmanan E (2012) Impact of Tanning Industries on Groundwater Quality near a Metropolitan  
513 City in India. *Water Resour. Manag.* 26: 1747-1761.

514 Kim YJ, Hamm S.-Y (1999) Assessment of the potential for groundwater contamination using the DRASTIC/EGIS  
515 technique, Cheongju area, South Korea. *Hydrogeol. J.* 7(2): 227-235.

516 Kumar A, Pramod Krishna A (2019) Groundwater vulnerability and contamination risk assessment using GIS-based  
517 modified DRASTIC-LU model in hard rock aquifer system in India. *Geocarto Int.* 35(11): 1149-1178.

518 Kumar S, Venkatesh AS, Singh R, Udayabhanu G, Saha D (2018) Geochemical signatures and isotopic systematics  
519 constraining dynamics of fluoride contamination in groundwater across Jamui district, Indo-Gangetic  
520 alluvial plains, India. *Chemosphere.* 205: 493-505.

521 Laerd Statistics: Lund Research Ltd. 2018. [accessed 2018 July 3]. <https://statistics.laerd.com/-spss-tutorials/spearman-rank-order-correlation-using-spss-statistics.php>.

523 Lakusic S (2019) Groundwater vulnerability mapping using modified DRASTIC ANP. *J. Croatian Assoc.Civ. Eng.*  
524 71(4): 283-296.

525 Lee S (2003) Evaluation of waste disposal site using the DRASTIC system in Southern Korea. *Environ. Geol.* 44(6):  
526 654-664.

527 Mahmoudzadeh E, Rezaian S, Ahmadi A (2013) Assessment of Meymeh Plain Aquifer Vulnerability in Esfahan  
528 Using Comparative Method AVI,GODS,DRASTIC. *J. Environ. Stud.* 39(2): 45-60.

529 Maqsoom A, Aslam B, Khalil U, Ghorbanzadeh O, Ashraf H, Faisal Tufail R, Farooq D, Blaschke T (2020) A GIS-  
530 based DRASTIC Model and an Adjusted DRASTIC Model (DRASTICA) for Groundwater Susceptibility  
531 Assessment along the China–Pakistan Economic Corridor (CPEC) Route. *Int. J. Geo-Inf.* 9.(5)

532 Martínez-Bastida JJ, Arauzo M, Valladolid M (2010) Intrinsic and specific vulnerability of groundwater in central  
533 Spain: the risk of nitrate pollution. *Hydrogeol. J.*, 18(3): 681-698.

534 Napolitano P, Fabbri A (1996) Single-parameter sensitivity analysis for aquifer vulnerability assessment using  
535 DRASTIC and SINTACS. IAHS-AISH Publication, 235: 559-566.

536 Natraj VM, Katyal D (2014) Study of fertilizer effect on soil status in and around Loni, Maharashtra, India. In:  
537 Proceedings of 3rd World Conference on Applied Sci. Engg. Tech. 188–192 (Kathmandu, Nepal).

538 Neshat A, Pradhan B (2017) Evaluation of groundwater vulnerability to pollution using DRASTIC framework and  
539 GIS. *Arab. J. Geosci.* 10(22): 501.

540 Noori R, Ghahremanzadeh H, Klove B, Adamowski JF, Baghvand A (2019) Modified-DRASTIC, modified-  
541 SINTACS and SI methods for groundwater vulnerability assessment in the southern Tehran aquifer. *J*  
542 *Environ Sci Health A Tox Hazard Subst Environ. Eng.* 54(1): 89-100.

543 Pacheco FAL, Pires LMGR, Santos RMB, Sanches Fernandes LF (2015) Factor weighting in DRASTIC modeling.  
544 *Sci. Total Environ.* 505: 474-486.

545 Panagopoulos GP, Antonakos AK, Lambrakis NJ (2006) Optimization of the DRASTIC method for groundwater  
546 vulnerability assessment via the use of simple statistical methods and GIS. *Hydrogeol. J.* 14(6): 894-911.

547 Pathak DR, Hiratsuka A, Awata I, Chen L (2009) Groundwater vulnerability assessment in shallow aquifer of  
548 Kathmandu Valley using GIS-based DRASTIC model. *Environ. Geol.* 57(7): 1569-1578.

549 Piscopo G (2001) Groundwater vulnerability map explanatory notes. Castlereagh Catchment, NSW. Department of  
550 Land and Water Conservation, Australia.

551 Saaty T (1980) *Multicriteria decision making : the analytic hierarchy process ; planning, priority setting, resource*  
552 *allocation.* New York McGraw-Hill 1988.

553 Saha D, Alam F (2014) Groundwater vulnerability assessment using DRASTIC and Pesticide DRASTIC models in  
554 intense agriculture area of the Gangetic plains, India. *Environ. Monit. Assess.* 186.

555 Sener E, Davraz A (2012) Assessment of groundwater vulnerability based on a modified DRASTIC model, GIS and  
556 an analytic hierarchy process (AHP) method: The case of Egirdir Lake basin (Isparta, Turkey). *Hydrogeol.*  
557 *J.*, 21.

558 Şener E, Şener Ş, (2015) Evaluation of groundwater vulnerability to pollution using fuzzy analytic hierarchy process  
559 method. *Environ. Earth Sci.* 73(12): 8405-8424.

560 Sener E, Şener Ş, Davraz A (2009) Assessment of aquifer vulnerability based on GIS and DRASTIC methods: A  
561 case study of the Senirkent-Uluborlu Basin (Isparta, Turkey). *Hydrogeol. J.* 17: 2023-2035.

562 Shirazi SM, Imran HM, Akib S, Yusop Z, Harun ZB (2013) Groundwater vulnerability assessment in the Melaka  
563 State of Malaysia using DRASTIC and GIS techniques. *Environ. Earth Sci.* 70(5): 2293-2304.

564 Simsek C, Kincal C, Gunduz O (2006) A solid waste disposal site selection procedure based on groundwater  
565 vulnerability mapping. *Environ. Geol.* 49(4): 620-633.

566 Sinha MK, Verma MK, Ahmad I, Baier K, Jha R, Azzam R (2016) Assessment of groundwater vulnerability using  
567 modified DRASTIC model in Kharun Basin, Chhattisgarh, India. *Arabian J. Geosci.* 9(2): 98.

568 Singha S, Pasupuleti S, Singha S, Villuri VGK (2017) An integrated approach for evaluation of groundwater quality  
569 in Korba district, Chhattisgarh using Geomatic techniques. *J. Environ. Bio.* 38(5): 865-872.

570 Stempvoort DV, Ewert L, Wassenaar L (1993) Aquifer Vulnerability Index: A Gis - Compatible Method for  
571 Groundwater Vulnerability Mapping. *Can. Water Resour. J.* 18(1): 25-37.

572 Tiwari AK, Singh PK, De Maio M (2016) Evaluation of aquifer vulnerability in a coal mining of India by using  
573 GIS-based DRASTIC model. *Arab. J. Geosci.* 9(6): 438.

574 Tomer T, Katyal D, Joshi V (2019) Sensitivity analysis of groundwater vulnerability using DRASTIC method: A  
575 case study of National Capital Territory, Delhi, India. *Groundw. Sustain. Dev.* 9.

576 Tseng M, Lin Y, Chiu A, Chen C (2008) Fuzzy AHP approach to TQM strategy evaluation. *IEMS* 7(1):34-43.

577 Umar R, Ahmed I, Alam F (2009) Mapping groundwater vulnerable zones using modified DRASTIC approach of  
578 an alluvial aquifer in parts of central Ganga plain, Western Uttar Pradesh. *J. Geolog. Soci. In.* 73(2): 193-  
579 201.

580 USEPA (1985) DRASTIC: a standard system for evaluating groundwater potential using hydrogeological settings.  
581 WA/EPA Series 1 ,985US EPA, Washington, DC, 163,pp.

582 van Laarhoven PJM, Pedrycz W (1983) A fuzzy extension of Saaty's priority theory. *Fuzzy Set. Syst.* 11(1): 229-  
583 241.

584 Vrba J, Zaporozec A (1994) Guidebook on mapping groundwater vulnerability, H. Heise, Hannover.

585 Wang Y, Merkel BJ, Li Y, Ye H, Fu S, Ihm D (2007) Vulnerability of groundwater in Quaternary aquifers to  
586 organic contaminants: a case study in Wuhan City, China. *Environ. Geo.* 53: 479.

# Figures

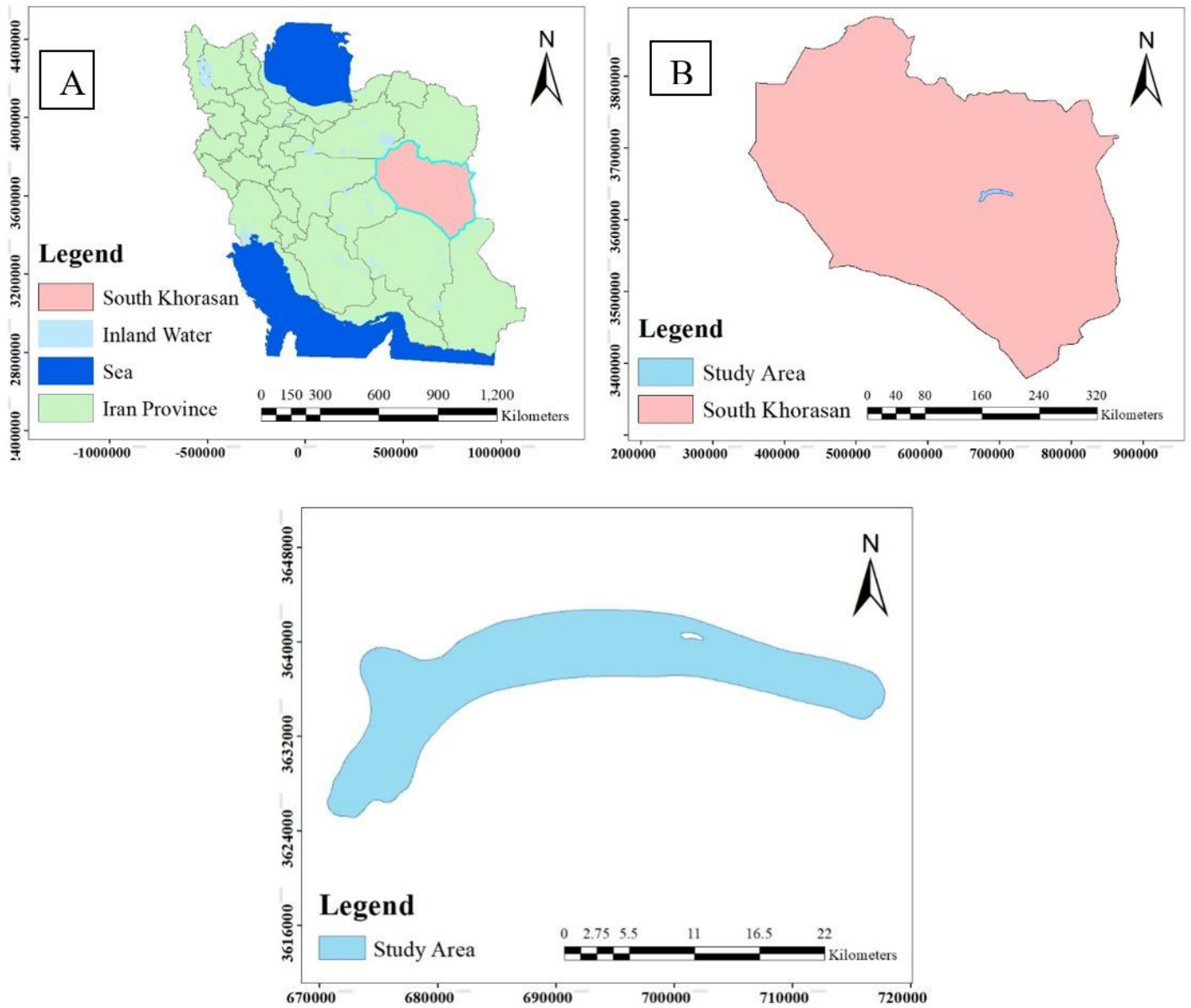


**Figure 1**

Location of the study area in Iran (A) and south Khorasan (B). Note: The designations employed and the presentation of the material on this map do not imply the expression of any opinion whatsoever on the part of Research Square concerning the legal status of any country, territory, city or area or of its authorities, or concerning the delimitation of its frontiers or boundaries. This map has been provided by the authors.

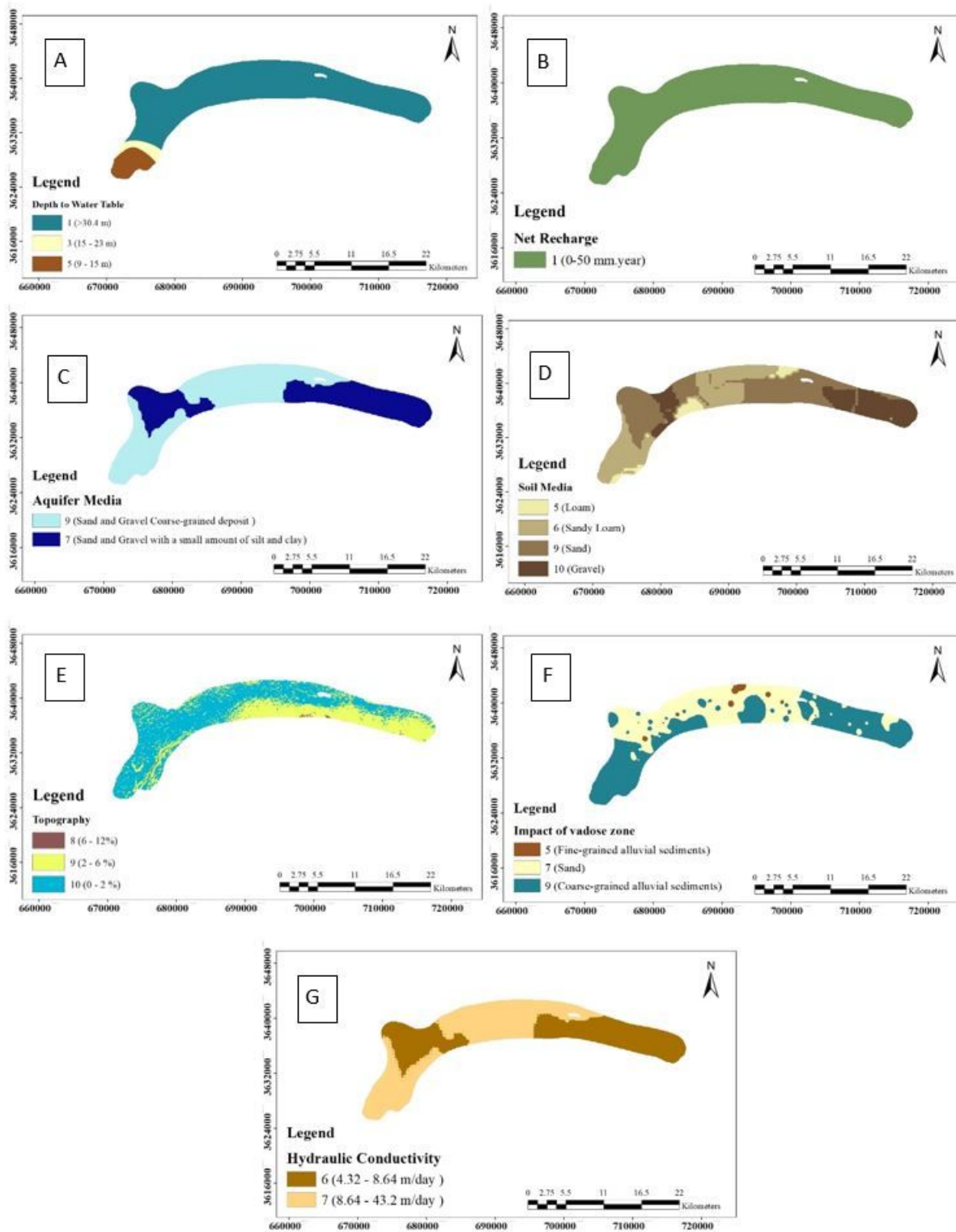


Figure 2

A) Water Depth; B) Net Recharge; C) Aquifer Media; D) Soil Media; E) Topography; F) Impact of vadose zone; G) Hydraulic conductivity

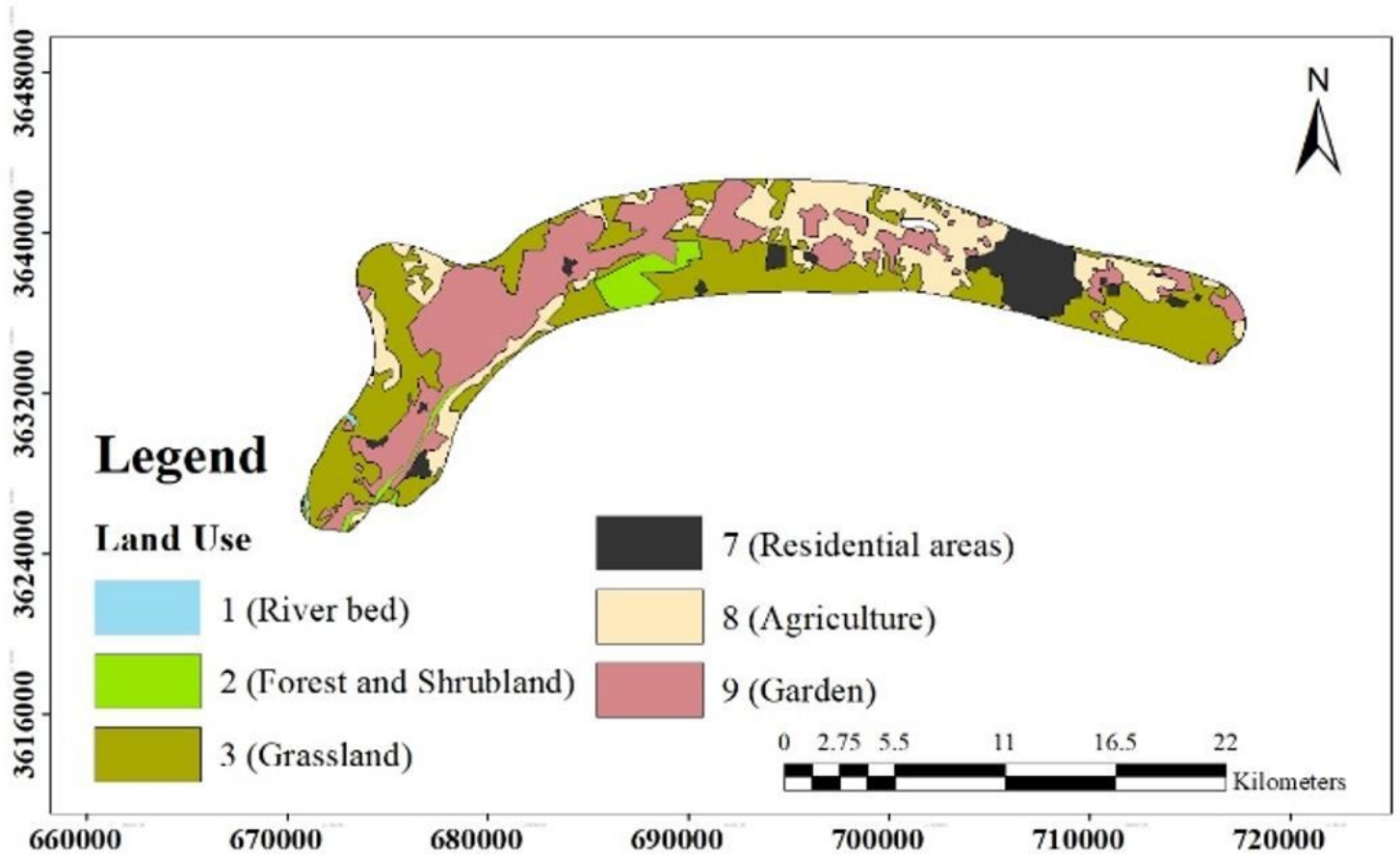


Figure 3

Land use map of the Birjand Plain

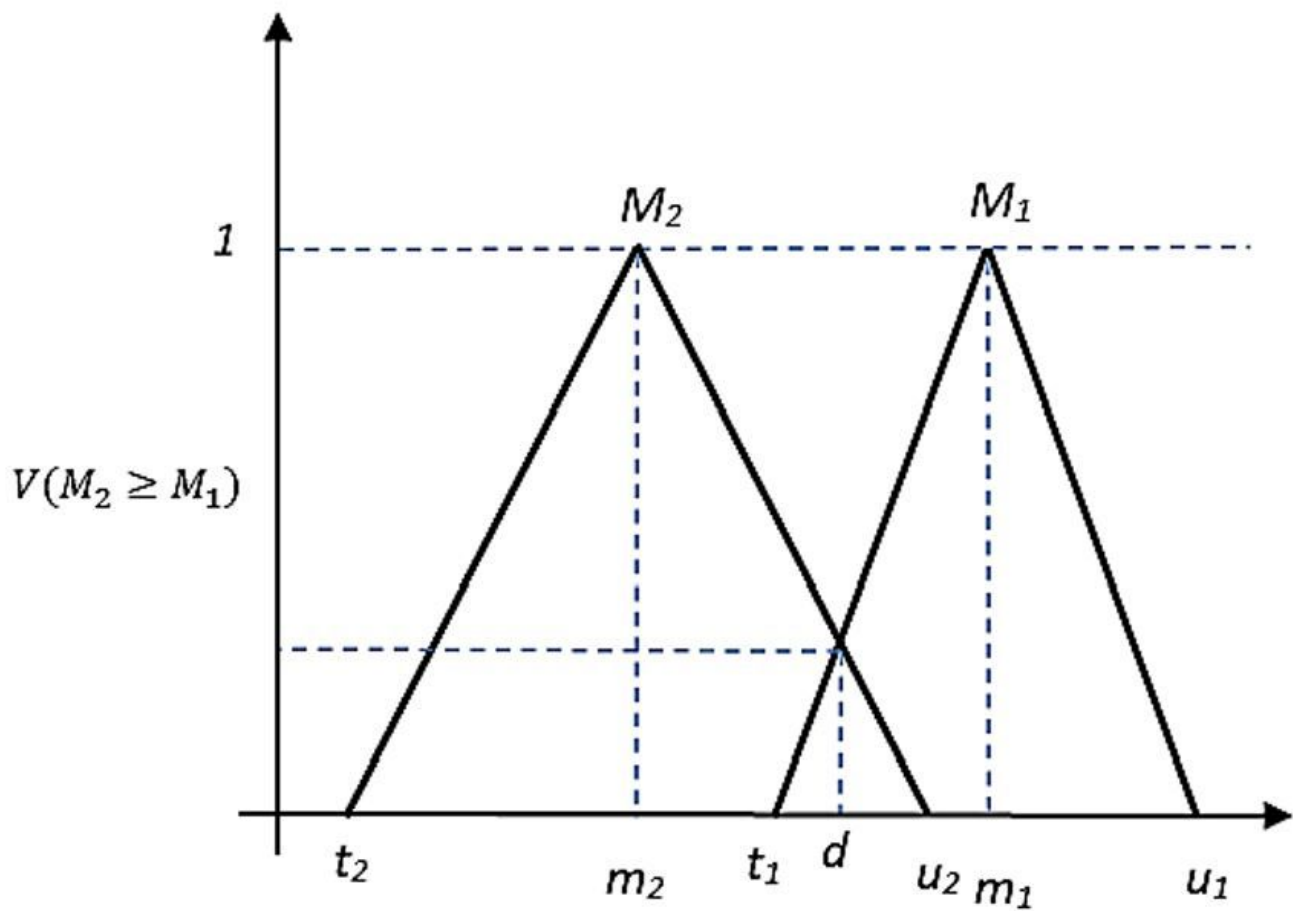


Figure 4

The intersection between M1 and M2 (Şener and Şener 2015)

Inconsistency: 0.02347

A	<div style="width: 25%; background-color: #00aaff;"></div>	0.15958
C	<div style="width: 15%; background-color: #00aaff;"></div>	0.09548
D	<div style="width: 35%; background-color: #00aaff;"></div>	0.26561
I	<div style="width: 20%; background-color: #00aaff;"></div>	0.12159
LU	<div style="width: 30%; background-color: #00aaff;"></div>	0.20334
R	<div style="width: 5%; background-color: #00aaff;"></div>	0.03735
S	<div style="width: 10%; background-color: #00aaff;"></div>	0.07357
T	<div style="width: 5%; background-color: #00aaff;"></div>	0.04348

Figure 5

Results of estimating the weights of MDRASTIC parameters in super decision

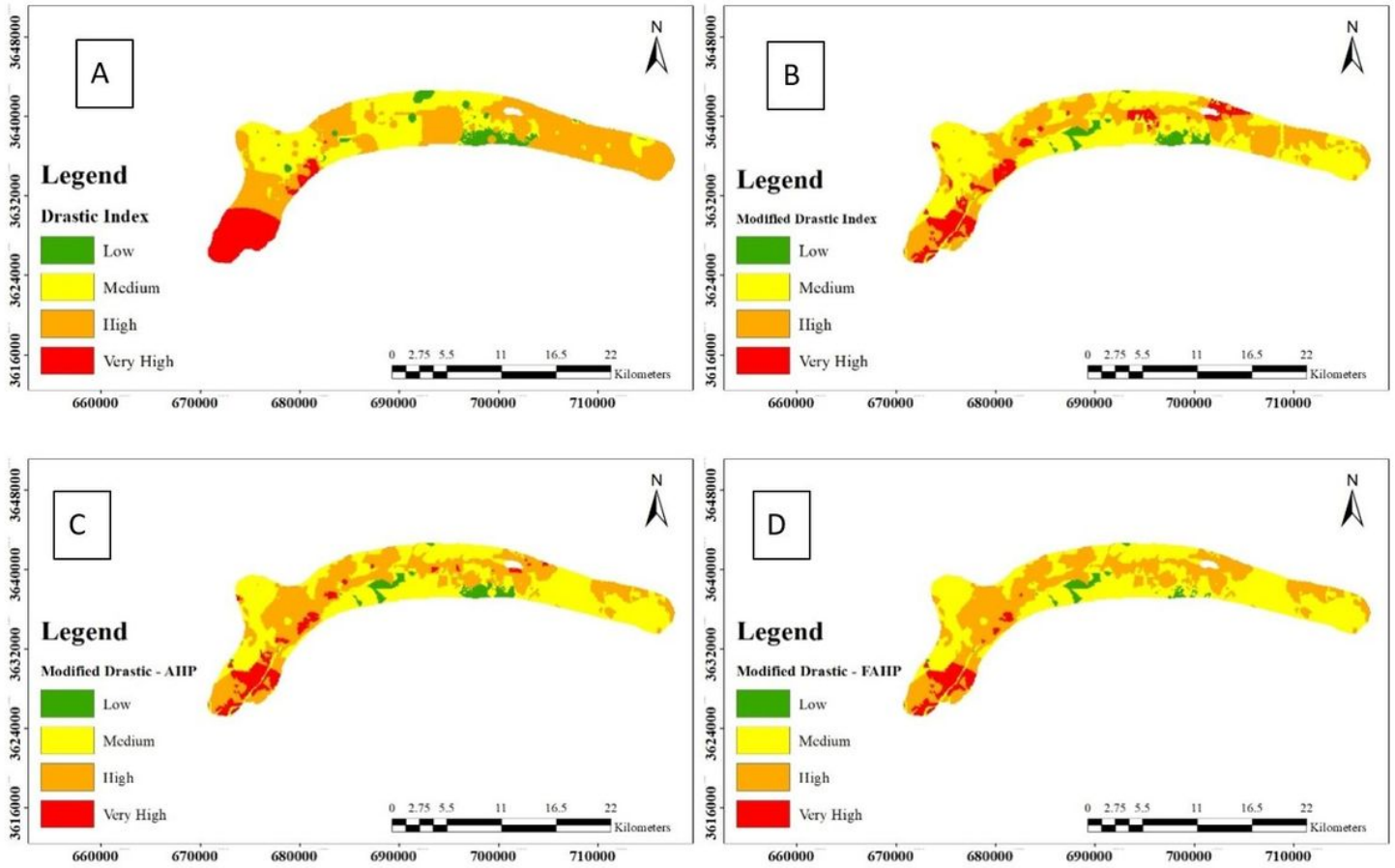


**Figure 6**

Groundwater vulnerability maps A) DRASTIC; B) MDRASTIC; C) MDRASTIC-AHP; D) MDRASTIC-FAHP

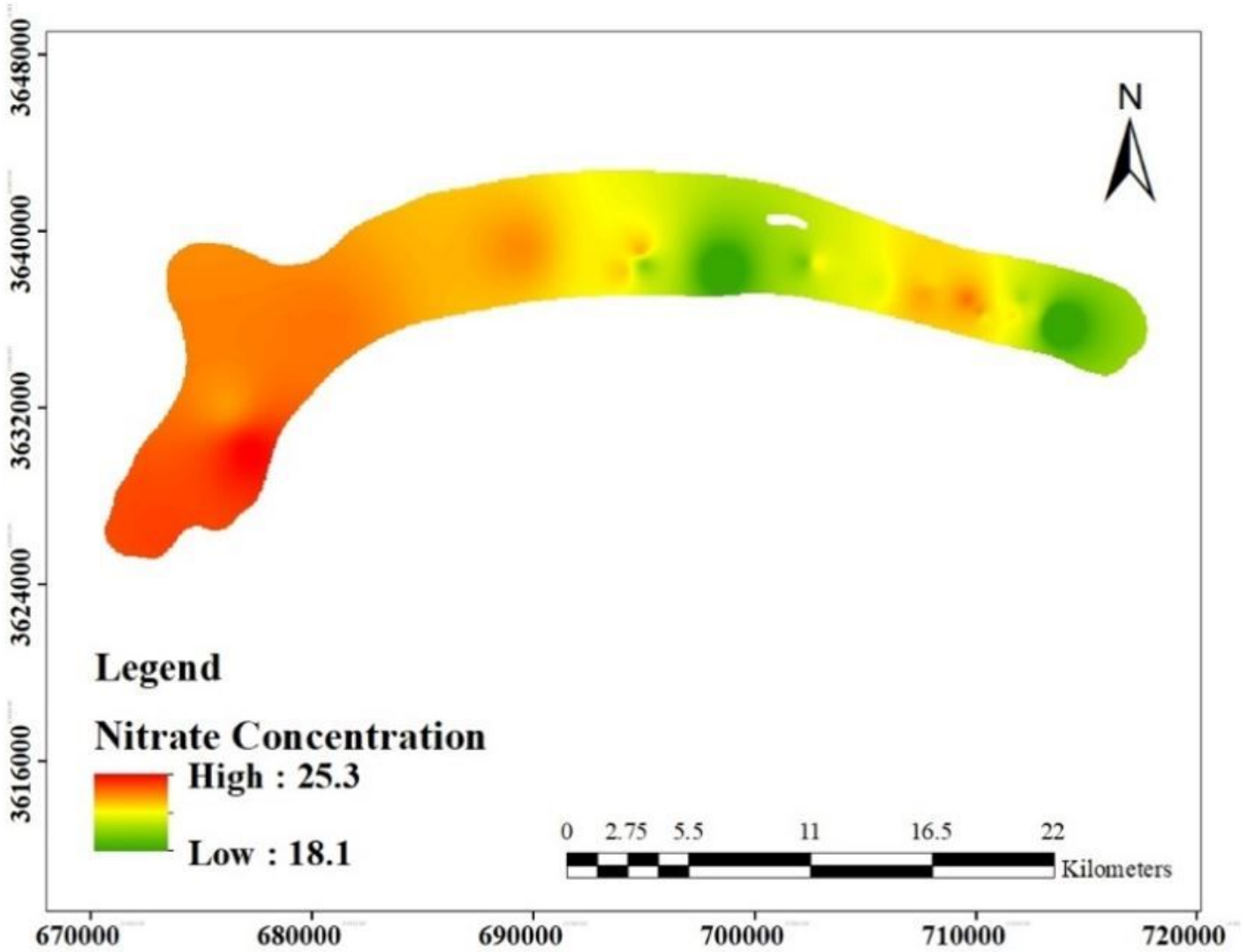
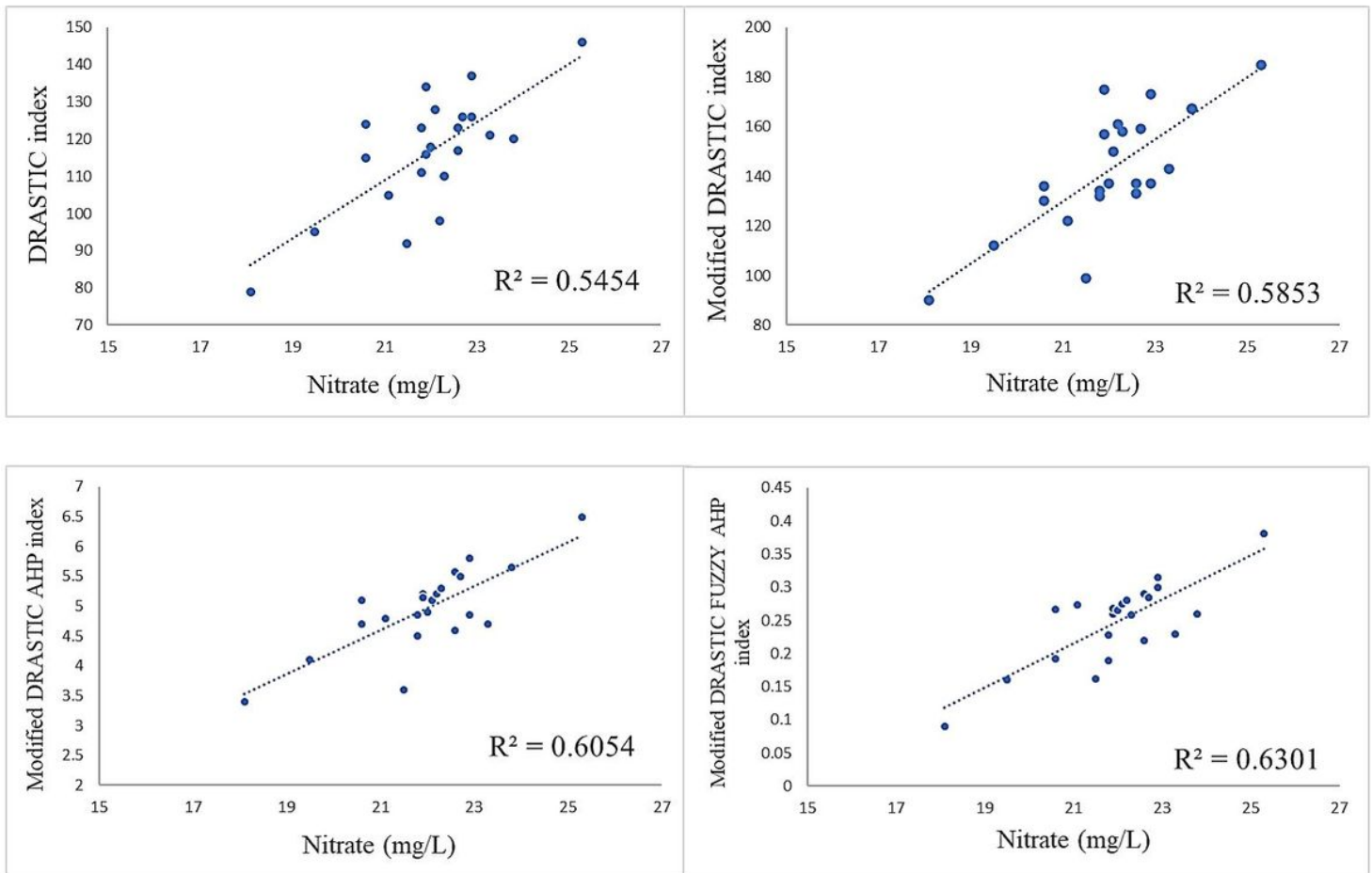


Figure 7

Nitrate concentration in groundwater of Birjand plain aquifer



**Figure 8**

Relationship between aquifer vulnerability maps obtained from each method and nitrate concentration:  
 A) DRASTIC, B) MDRASTIC, C) MDRASTIC-AHP D) MDRASTIC-FAHP

## Supplementary Files

This is a list of supplementary files associated with this preprint. Click to download.

- [GraphicalAbstractOriginal1.docx](#)
- [HighlightsOriginal.docx](#)